

# Stacking-fault energies for Ag, Cu, and Ni from empirical tight-binding potentials

R. Meyer\* and L. J. Lewis†

*Département de physique et Groupe de recherche en physique et technologie des couches minces (GCM),  
Université de Montréal, C.P. 6128 Succursale Centre-ville, Montréal (Québec) H3C 3J7, Canada*

(Dated: July 12, 2002)

The intrinsic stacking-fault energies and free energies for Ag, Cu, and Ni are derived from molecular-dynamics simulations using the empirical tight-binding potentials of Cleri and Rosato [Phys. Rev. B **48**, 22 (1993)]. While the results show significant deviations from experimental data, the general trend between the elements remains correct. This allows to use the potentials for qualitative comparisons between metals with high and low stacking-fault energies. Moreover, the effect of stacking faults on the local vibrational properties near the fault is examined. It turns out that the stacking fault has the strongest effect on modes in the center of the transverse peak and its effect is localized in a region of approximately eight monolayers around the defect.

PACS numbers: 61.72.Nn, 63.20.Dj, 02.70.Ns

## I. INTRODUCTION

The stacking-fault energy is an important property of a material since it determines to a high degree its deformation and failure behavior.<sup>1</sup> Therefore, for the computer modeling of processes involving plastic deformation and/or failure, a correct representation of the stacking-fault energy by the employed model is desirable. However, many models have been constructed without consideration of stacking-fault energies and the predicted values deviate often considerably from experimental results.<sup>2,3,4</sup> A precise knowledge of the stacking-fault energies predicted by empirical models is therefore of high interest in order to correctly interpret results of computer simulations.

The empirical tight-binding potentials of Cleri and Rosato<sup>5</sup> are extensively used in atomistic simulations since they give a reasonable description of many structural and thermal properties of fcc metals. In this work we study the intrinsic stacking-fault energies and free energies predicted by these potentials for Ag, Cu, and Ni and compare them with the results of similar models for Cu and Ni. The stacking-fault energies were calculated at  $T = 300$  K from molecular-dynamics simulations and at  $T = 0$  K with the help of relaxation calculations (molecular-statics). The derivation of the vibrational density of states (VDOS) from the simulations made it also possible for us to calculate the stacking-fault free energies within the quasiharmonic approximation and to study the local effect of stacking-faults in fcc metals.

The aim of this paper is to provide the stacking-fault energies for Ag, Cu, and Ni modeled by the potentials of Cleri and Rosato. We expect that these values will contribute to proper discussions of results based on these potentials. Although in the case of Ag and Cu the values derived from the simulations are significantly lower than the experimental results, the trend between all three elements is well reproduced. It has to be noted that the occurrence of low stacking-fault energies is a general problem of central-force potentials. One reason for this is that without the consideration of angular forces sig-

nificant contributions to the stacking-fault energy arise from the third and higher neighbor shells, only.<sup>6</sup> A related explanation is given by the nearest neighbor d-band tight-binding model where the energy difference between the fcc and hcp structure is dominated by the fifth and sixth moment of the density of states,<sup>7</sup> whereas many empirical potentials, including those of Cleri and Rosato, are based on the second moment approximation. Better agreements of computationally simple empirical potentials with experimental values for the stacking-fault energy require therefore the explicit consideration of the stacking-fault energy during the construction of the potentials.

## II. COMPUTATIONAL METHODS

### A. General

As stated in the introduction, the stacking-fault energies and free energies reported in this article have been derived from molecular-dynamics simulations employing the potentials of Cleri and Rosato.<sup>5</sup> In these simulations the equations of motions have been integrated with the help of the velocity form of the Verlet-algorithm<sup>8</sup> using a time-step of 2 fs. Isothermic-isochoric (NVT ensemble) and isobaric-isoenthalpic (NpH ensemble) conditions were achieved where necessary by the application of the Nosé-Hoover thermostat<sup>9</sup> method and the Parrinello-Rahman scheme<sup>10</sup> (restricted to orthogonal simulation boxes), respectively. Periodic boundary conditions were applied in all cases.

Calculations of the relaxed structures at  $T = 0$  K were done in two steps. First, the systems were cooled down to a temperature of  $T = 0.1$  K. Afterwards, the final configurations were obtained with the help of a steepest-descent method.

For each of the three elements a stacking-fault configuration and a reference configuration were prepared. The stacking-fault configurations were composed as a stack of 110 triangular lattice layers building a nearly cubic sys-

tem of  $N_{\text{st}} = 1\,018\,160$  atoms with one stacking-fault; the reference configurations on the other hand are regular fcc systems  $N_{\text{fcc}} = 1\,000\,188$  atoms ( $63^3$  cubic cells).

At first glance, configurations with more than a million atoms may seem to be exaggerated for the simple calculation of stacking-fault energies. However, these system sizes guarantee the presence of a sufficiently large number of vibrational modes for the calculations of free energies in the quasiharmonic approximation. In addition, the large system sizes lead to large distances between the periodic copies of the stacking-fault, thereby minimizing possible self-interaction effects.

Before the calculation of the stacking-fault energies could begin, the equilibrium dimensions of all configurations had to be determined at  $T = 0$  and 300 K. In the case of the reference configurations these were derived from the  $T = 0$  K lattice constants given in Ref. 5 and the average system volumes obtained from isobaric-isoenthalpic simulations at  $T = 300$  K and zero pressure.

For the determination of the equilibrium sizes of the stacking-fault configurations, it had to be taken into account that only volume relaxations perpendicular to the plane of the stacking fault are physically relevant. Relaxations in the directions parallel to the fault-plane are artifacts of the finite system size and diminish if the number of atomic layers parallel to the fault is increased. For this reason the in-plane dimensions of the simulation boxes of the stacking-fault configurations were derived from the lattice constants obtained for the perfect systems and only the out-of-plane dimensions had to be explicitly determined. At  $T = 300$  K these missing dimensions were again obtained with the help of zero-pressure isobaric-isoenthalpic simulations in which only the out-of-plane direction of the simulation box was allowed to fluctuate. Similarly the volume relaxations at  $T = 0$  K were derived from relaxations of the stacking-fault configurations with fixed in-plane dimensions of the simulation box.

## B. Calculation of stacking-fault energies

After the dimensions of the configurations had been determined, the stacking-fault energies  $\gamma$  of the three metals could be obtained. For this the simple formula

$$\gamma = \frac{N_{\text{sf}}(e_{\text{sf}} - e_{\text{fcc}})}{A}, \quad (1)$$

was used, where  $A$  is the area of the stacking-fault plane,  $N_{\text{sf}}$  the number of atoms in the stacking-fault configuration and  $e_{\text{sf}}$ ,  $e_{\text{fcc}}$  the potential energies per atom in the respective configuration. The kinetic energy does not contribute to the stacking-fault energy since its per particle value does not depend on the configuration.

Particular attention has to be paid to the system temperature. The usual method to attain the desired temperature in molecular-dynamics simulations is to rescale the particle velocities repeatedly until the system is equilibrated. In simulations run under conditions of constant

energy or enthalpy, this procedure may lead to a small offset in the temperature which in turn affects the value of the potential energy. While these discrepancies usually are very small and can be neglected in most cases, they can have a dramatic impact on the values of  $\gamma$  since the potential energy difference on the right hand side of Eq. (1) is much smaller than the potential energies themselves and can be comparable to — or even smaller than — the error in the potential energies induced by temperature deviations. In order to avoid this problem we derived the potential energies from simulations in the canonical (NVT) ensemble.

## C. Calculation of stacking-fault free energies

The exact calculation of free energies from molecular-dynamics simulations is a difficult task. In this work we employ the quasiharmonic approximation<sup>11</sup> to derive the free energies  $F$  of the stacking-fault and reference configurations. Within this approach the free energy is given by

$$F = E_0(V) + 3N \int_0^\infty g(\omega) \left[ \frac{\hbar\omega}{2} + \frac{1}{\beta} \log(1 - e^{-\beta\hbar\omega}) \right] d\omega, \quad (2)$$

where  $\beta$  is the inverse temperature  $(k_{\text{B}}T)^{-1}$ ,  $g(\omega)$  the normalized VDOS and  $E_0(V)$  denotes the ground-state energy of the system *for the equilibrium volume at temperature  $T$* . In contrast to most molecular-dynamics simulations, Eq. (2) takes quantum effects fully into account. However, since we are mainly interested in the values of the stacking-fault energies in a classical computer-simulation context, it is more appropriate to calculate the free energy in the classical limit. Taking this limit and neglecting the purely quantum zero-point fluctuations, Eq. (2) becomes

$$F_{\text{cl}} = E_0(V) + 3N\beta^{-1} \int_0^\infty g(\omega) \log(\beta\hbar\omega) d\omega. \quad (3)$$

Given Eq. (3) the task of calculating the free energy of the configurations by molecular-dynamics simulations reduces to the determination of the vibrational density of states  $g(\omega)$  and the ground-state energy  $E_0(V)$ . The latter quantity was obtained by a relaxation of the systems to  $T = 0$  K using the simulation box dimensions of  $T = 300$  K. In order to derive the vibrational density of states  $g(\omega)$ , simulations in the NVE ensemble were performed at  $T = 300$  K. From the trajectories of the particles during these simulations the velocity-autocorrelation function  $\langle \mathbf{v}(t)\mathbf{v}(0) \rangle$  was derived which is related to the normalized VDOS by<sup>12</sup>

$$g(\omega) = \int_{-\infty}^\infty \frac{\langle \mathbf{v}(t)\mathbf{v}(0) \rangle}{\langle \mathbf{v}(0)\mathbf{v}(0) \rangle} e^{i\omega t} dt. \quad (4)$$

In order to reduce statistical errors, the density of states  $g(\omega)$  was averaged over ten or more simulation runs of

5000 steps, each. From the density of states obtained this way the free energies of all six configurations could be calculated with the help of Eq. (3). These values were then used to calculate the intrinsic stacking-fault free energies  $\tilde{\gamma}$  of the three elements by replacing the potential energies per particle in Eq. (1) by the corresponding free energies per particle. Since at  $T = 0$  K energy and free energy are identical these calculations had to be done only at  $T = 300$  K.

### III. RESULTS

#### A. Stacking-fault Energies

In Table I we present the stacking-fault energies and free energies obtained from molecular-dynamics simulations as described in the preceding section. From this table it can be seen that the general agreement with the experimental results is only qualitative, similar to comparable models. The calculated stacking-fault energies (and free energies) for Cu and Ag are much smaller than their experimental counterparts; the calculated stacking-fault free energy of Ag at room temperature is even negative. For Ni the situation is not clear due to the large variation of the experimental data. However, the trend among the three elements is well reproduced by the model. This means that while one has to be careful with the interpretation of quantitative results, the potentials of Cleri and Rosato are well suited for comparisons between materials with high, low and very low stacking-fault energies.

In accordance with the experimental data,<sup>17</sup> the results in Table I show a decrease of the stacking-fault energies and free energies with increasing temperature. In the case of the stacking-fault energies, the decrease is caused by anharmonic effects only, since the specific heat of a purely harmonic, classical system does not depend on structural details. In contrast to this, the decrease of the stacking-fault free energies in Table I contains har-

TABLE I: Experimental (*e*) and theoretical (*t*) values of stacking-fault energies for Ag, Cu, and Ni (in mJ/m<sup>2</sup>).  $\gamma$  and  $\tilde{\gamma}$  are the stacking-fault energies and free energies obtained in this work; OJ and VC denote the values given in Ref. 3 for the models of Oh and Johnson<sup>13</sup> and Voter and Chen.<sup>14,15</sup> The experimental results are taken from the compilations of Gallagher<sup>16</sup> and Murr.<sup>17</sup>

		<i>T</i>	Ag	Cu	Ni
$\gamma$	( <i>t</i> )	0 K	1	21	305
$\gamma$	( <i>t</i> )	300 K	0	15	262
$\tilde{\gamma}$	( <i>t</i> )	300 K	-2	14	292
OJ	( <i>t</i> )	0 K		27	13
VC	( <i>t</i> )	0 K		37	87
Gallagher	( <i>e</i> )		22	55	250
Murr	( <i>e</i> )	300 K	22	78	128

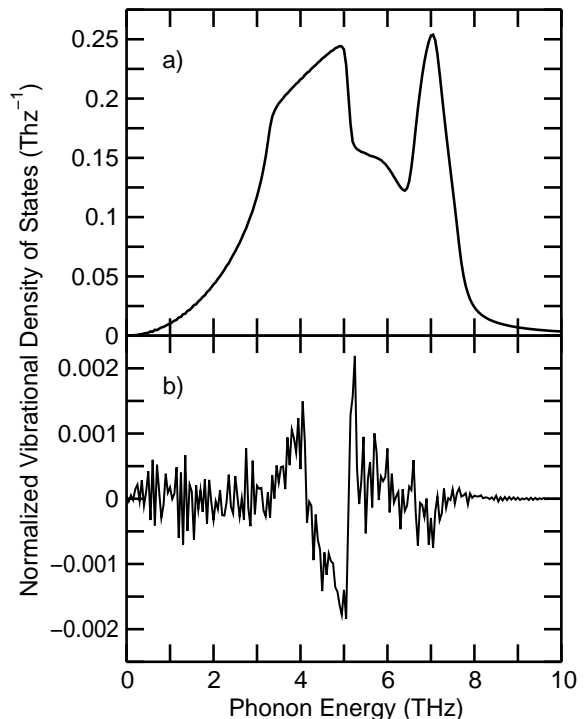


FIG. 1: a) Calculated normalized VDOS  $g_{fcc}(\omega)$  for crystalline fcc Cu. b) Difference  $\Delta g(\omega) = g_{sf}(\omega) - g_{fcc}(\omega)$  between the VDOS  $g_{sf}(\omega)$  of the system with stacking-fault and  $g_{fcc}(\omega)$ .

monic and anharmonic contributions. However, due to the nature of the quasiharmonic approximation, the anharmonic contributions are treated only in an approximate fashion via the volume dependence of  $E_0$  and the temperature dependence of the VDOS. This approximation gets in the way if one wants to compare the stacking-fault energies and free energies in order to determine the role of entropic contributions to the stacking-fault energy. Particularly striking is the large discrepancy between the stacking-fault energy and free energy of Ni at room temperature. Since our results indicate that the entropy difference favors the stacking-fault configuration, the stacking-fault free energy should be the lower quantity, as it is the case for Cu and Ag. This shows that, at least in the case of Ni, there are important anharmonic contributions to the stacking-fault free energy which are not accounted for by the quasiharmonic approximation.

#### B. Vibrational Density of States

Figure 1 shows the VDOS calculated for the fcc structure as well as the difference of the VDOS between the stacking-fault and the perfect fcc configuration. It should be noted that the absolute value of this difference is physically irrelevant since it depends on the system size and goes to zero in the limit of an infinitely thick system. However, the shape of this function is system size independent and reveals the energy regions where the VDOS

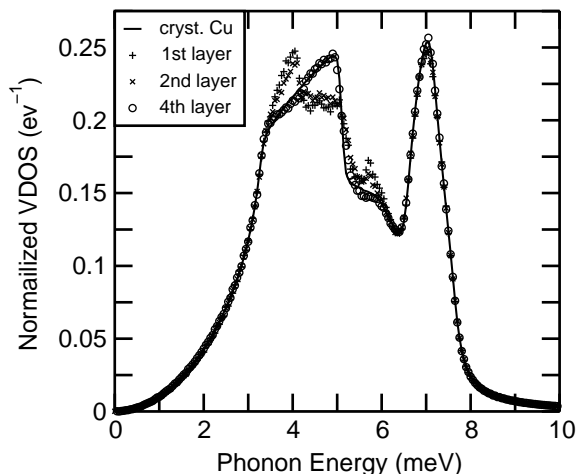


FIG. 2: Normalized local VDOS of the atoms in the first, second, and fourth layer away from a stacking fault in Cu compared to the VDOS in the perfect crystal.

is affected by the stacking fault. From the lower panel of Fig. 1 it can be seen that the strongest effect of the stacking fault appears in the transverse peak where modes are transferred from the center of the peak to (mostly) lower energies. A similar but smaller transfer takes place in the longitudinal peak. It is these transfers which give rise to the entropy difference between the configurations, which in turn accounts for the temperature dependent change of the stacking-fault free energy within the quasiharmonic approximation. A similar behavior is found for Ag and Ni with a slightly more pronounced transfer of longitudinal modes in the case of Ni.

In order to see the spatial extent of the influence of stacking faults on the vibrational properties of the crystal lattice we have calculated the local VDOS for the first atomic layers near a stacking fault in Cu. The results of this calculation, which are presented in Fig. 2, show that atoms in the first and second layer near the fault account for most of the change of the total VDOS in Fig. 1, whereas the VDOS in the fourth layer differs only slightly from the bulk VDOS. Atoms in the third layer (whose VDOS is not given in order to avoid overcrowding of the figure) have an intermediate character. While their VDOS is still clearly different from the VDOS of the crystalline bulk, it is already much closer to this than to the VDOS of the first two layers.

#### IV. SUMMARY AND CONCLUSIONS

The stacking-fault energies predicted by the empirical tight-binding potentials of Cleri and Rosato reflect

the experimental values of Ag, Cu, and Ni qualitatively. Similar to other empirical models they underestimate the values of Ag and Cu. In contrast to this and in rough agreement with experimental data, rather high stacking-fault energies are found for Ni. Since the experimental data for Ni show strong variations it is impossible to say whether the potential for this metal overestimates the stacking-fault energy or not. In any case, the potentials can be used for qualitative comparisons of materials with high, low, and very low stacking-fault energies.

For all three metals we find a decrease of the stacking-fault energy with increasing temperature of the same order of magnitude as it is experimentally observed.<sup>17</sup> This decrease has to be considered in the construction or evaluation of models which explicitly take the stacking-fault energies into account.

The discrepancy between the calculated room temperature stacking-fault energy and free energy for Ni shows that important anharmonic effects are missed by the quasiharmonic approximation. For this reason one should not put too much emphasis on the negative value found for the room temperature stacking-fault free energy of Ag. What remains is the question why the anharmonic effects are so much stronger for Ni. A possible explanation might be given by the relative importance of the many-body term vs. the pair-potential term in the model. An inspection of the parameters of the potentials in Ref. 5 shows indeed that the pair-potential term has a lower weight and a shorter range for Ni than for Cu or Ag. Thus, the increased weight of the many-body term in the case of Ni might account for the increased occurrence of anharmonic effects in this metal.

Finally, the analysis of the local effect of stacking-faults on the vibrational properties in fcc metals reveals a strong transfer of modes to lower energies in the transverse peak and a similar but less pronounced transfer in the longitudinal peak of the VDOS. Inspection of the layer-resolved local VDOS shows that these effects are localized in a region of six to eight monolayers around the defect.

#### Acknowledgments

This work has been supported by grants from the Canadian Natural Sciences and Engineering Research Council (NSERC), Québec's *Fonds pour la formation de chercheurs et l'aide à la recherche* (FCAR) and Germany's *Deutsche Forschungsgemeinschaft* (DFG). Most of the calculations have been performed on the facilities of the *Réseau québécois de calcul de haute performance* (RQCHP).

\* Electronic address: ralf@thp.uni-duisburg.de; Present address: Institut für Physik, Gerhard-Mercator-Universität

Duisburg, Lotharstraße 1, D-47048 Duisburg, Germany

- <sup>†</sup> Electronic address: Laurent.Lewis@UMontreal.CA
- <sup>1</sup> J. P. Hirth and J. Lothe, *Theory of Dislocations* (McGraw-Hill, New-York, 1968).
- <sup>2</sup> P. Heino, L. Perondi, K. Kaski, and E. Ristolainen, *Phys. Rev. B* **60**, 14625 (1999).
- <sup>3</sup> J. A. Zimmerman, H. Gao, and F. F. Abraham, *Modelling Simul. Mater. Sci. Eng.* **8**, 103 (2000).
- <sup>4</sup> M. J. Mehl, D. A. Papaconstantopoulos, N. Kioussis, and M. Herbranson, *Phys. Rev. B* **61**, 4894 (2000).
- <sup>5</sup> F. Cleri and V. Rosato, *Phys. Rev. B* **48**, 22 (1993).
- <sup>6</sup> A. Girshick, D. G. Pettifor, and V. Vitek, *Phil. Mag. A* **77**, 999 (1998).
- <sup>7</sup> A. P. Sutton, *Electronic Structure of Materials* (Clarendon, Oxford, 1993), chap. 9.
- <sup>8</sup> M. P. Allen and D. J. Tildesley, *Computer Simulations of Liquids* (Clarendon, Oxford, 1991).
- <sup>9</sup> W. G. Hoover, *Phys. Rev. A* **31**, 1695 (1985).
- <sup>10</sup> M. Parrinello and A. Rahman, *Phys. Rev. Lett.* **45**, 1196 (1980).
- <sup>11</sup> L. J. Lewis and M. L. Klein, in *Dynamical Properties of Solids*, edited by G. K. Horton and A. A. Maradudin (Amsterdam, 1990), vol. 6.
- <sup>12</sup> S. W. Lovesey, *Condensed matter physics: dynamic correlations*, vol. 61 of *Frontiers in Physics* (Benjamin/Cummings, Menlo Park, Calif., 1986).
- <sup>13</sup> D. J. Oh and R. A. Johnson, *J. Mater. Res.* **3**, 471 (1988).
- <sup>14</sup> A. F. Voter and S. P. Chen, *Mat. Res. Soc. Proc.* **82**, 175 (1987).
- <sup>15</sup> A. F. Voter, in *Intermetallic Compounds: Principles and Practice* (Wiley, New York, 1995), vol. 1, pp. 77–90.
- <sup>16</sup> P. C. J. Gallagher, *Met. Trans.* **1**, 2429 (1970).
- <sup>17</sup> L. E. Murr, *Interfacial Phenomena in Metals and Alloys* (Addison Wesley, Reading MA, 1975).